Dynamics of scalar fields in the background of rotating black holes

William Krivan
Institut für Astronomie und Astrophysik, Universität Tübingen, D-72076 Tübingen, Germany
and Department of Astronomy and Astrophysics and Center for Gravitational Physics and Geometry, Pennsylvania State University, University Park, Pennsylvania 16802

Pablo Laguna and Philippos Papadopoulos
Department of Astronomy and Astrophysics and Center for Gravitational Physics and Geometry, Pennsylvania State University, University Park, Pennsylvania 16802

(Received 4 June 1996)

A numerical study of the evolution of a massless scalar field in the background of rotating black holes is presented. First, solutions to the wave equation are obtained for slowly rotating black holes. In this approximation, the background geometry is treated as a perturbed Schwarzschild spacetime with the angular momentum per unit mass playing the role of a perturbative parameter. To first order in the angular momentum of the black hole, the scalar wave equation yields two coupled one-dimensional evolution equations. In this approximation, the late time dynamics of a massless scalar field exhibit the same power-law behavior as in the case of a Schwarzschild background. Solutions to the wave equation are also obtained for rapidly rotating black holes. In this case, owing to higher order terms in the angular momentum, the wave equation does not admit complete separation of variables and yields a two-dimensional evolution equation. The study shows that, depending on initial conditions, the late-time dynamics of a massless scalar field is dominated by the lowest-allowed mode with respect to l for a fixed value of m. [S0556-2821(96)02920-7]

PACS number(s): 04.30.Nk, 04.25.Dm, 04.70.Bw

I. INTRODUCTION

Perhaps the simplest wave phenomenon in relativity is the propagation of linearized waves on a fixed, curved background. When observed at a fixed spatial point, the dynamics of a wave propagating on spherically symmetric, time-independent, asymptotically flat, background geometries consists of three stages. During the first stage, the observed wave depends on the structure of the initial pulse and its reflection from the origin (burst phase). This phase is followed by an exponentially decaying quasinormal ringing of the black hole (quasinormal phase). In the last stage, the wave slowly dies off as a power-law tail (tail phase). The last two phases are dictated by the interference of the part of the wave backscattered at the tail of the potential and the part reflected by the potential barrier.

The tail phenomenon can be understood as due to the scattering of the wave off the effective curvature potential of the background geometry [1,2]. Tails have been mostly investigated on Schwarzschild backgrounds [3–5], Reissner-Nordström black holes [5], and for collapsing scalar fields [6,7]. The study of tails has also implications in connection with the gravitational radiation emerging from inspiraling binary systems [8].

For stationary spherically symmetric systems, after separation of variables, the three-dimensional wave equation $\nabla_\mu \nabla^\mu \Phi = 0$ reduces, in a suitable radial coordinate x, to the one-dimensional wave equation

$$[-\partial_t^2 + \partial_x^2 - V(x)]\Phi(x,t) = 0, \tag{1}$$

where $V(x)$ denotes the effective curvature potential. Recently, the late-time behavior of Eq. (1) has been the subject of detailed numerical and analytic investigations by Gundlach *et al.* [5] and Ching *et al.* [3,4].

Gundlach *et al.* [5,7] studied both the late-time behavior of massless fields around a fixed Schwarzschild geometry and the full nonlinear evolution of a minimally coupled scalar field. Their studies show a remarkable agreement between the numerically computed quasinormal frequencies and power-law tails and their corresponding theoretical predictions. Using a characteristic initial value approach, they found tails not only at timelike infinity, but also at future null infinity and at the future horizon of the black hole. The time behavior of the tails is shown to be

$$\Phi \sim \begin{cases} t^{-(2l+P+1)} & \text{at timelike infinity,} \\ (t-x)^{-(l+P)} & \text{at future null infinity,} \\ (t+x)^{-(2l+P+1)} & \text{at the future horizon,} \end{cases} \tag{2}$$

with $P=1$ if there is an initial static field and $P=2$ otherwise.

Pursuing a different approach, Ching *et al.* [3,4] showed that the late time tail phenomena are governed by the asymptotic structure of the background spacetime. Furthermore, they found that, for nonstatic initial conditions, the simple power-law $\Phi \sim t^{-2l+\alpha}$ in Schwarzschild geometries, is not present for general potentials of the form $V(x) \sim l(l+1)/x^2 + x^{-\alpha}\ln x$. Instead, the generic late-time behavior is given by $\Phi \sim t^{-2l+\alpha}\ln t$.

In spite of previous work, a complete understanding of the tail phenomenon for general systems is still missing. Questions such as which factors determine the magnitude and

power-law time dependence have not been addressed for a general system. It is of particular interest, for instance, to show which role the dimensionality of the system plays on the existence of power-law tails [9]. When the point of view that tails arise from backscattering off an effective potential is adopted, it is not clear whether the tail behavior would remain unchanged, or be present at all, for intrinsically two- or three-dimensional systems [10].

A natural generalization of previous studies to axisymmetric spacetimes is obtained by considering the family of Kerr spacetimes. In contrast with the Schwarzschild background geometry, the wave equation $\nabla_\mu \nabla^\mu \Phi = 0$ in the background of a rotating black hole only admits separation of the azimuthal coordinate, so in principle a two-dimensional evolution problem has to be solved. It has been suggested [3] that tails similar to those present in Schwarzschild spacetimes should exist on Kerr backgrounds, a detailed analysis, however, has not been undertaken.

This study considers the dynamics of scalar fields on the background of rotating black holes in two regimes: slowly and rapidly rotating holes. A considerable mathematical simplification of the problem is achieved in the case of slowly rotating black holes since the angular momentum can be treated as a perturbative parameter. Thus, to first order in the angular momentum, the scalar wave equation yields two one-dimensional evolution equations. This formalism is described in Sec. II. Results of the numerical calculations are presented in Sec. III, where power-law tails are discussed. The case of rapidly rotating black holes is discussed in Sec. IV.

II. SLOWLY ROTATING BLACK HOLES

Using Boyer-Lindquist coordinates (t, r, θ, ϕ), the wave equation for a massless scalar field Φ reads [11]

$$-\left[\frac{(r^2+a^2)^2}{\Delta} - a^2 \sin^2\theta\right]\partial_{tt}\Phi - \frac{4Mar}{\Delta}\partial_{t\phi}\Phi + \left[\frac{1}{\sin^2\theta} - \frac{a^2}{\Delta}\right]\partial_{\phi\phi}\Phi + \partial_r(\Delta\partial_r\Phi) + \frac{1}{\sin\theta}\partial_\theta(\sin\theta\partial_\theta\Phi) = 0, \tag{3}$$

where M is the mass of the black hole, a is its angular momentum per unit mass, and $\Delta \equiv r^2 - 2Mr + a^2$. Equation (3) is equivalent to the special case of the Teukolsky equation [12] for fields with vanishing spin weight.

The Schwarzschild case, $a = 0$, allows separation of variables in terms of the scalar spherical harmonics $Y_l^m(\theta, \phi)$ without any requirements on a particular time behavior. The solution of Eq. (3) can be written in the form

$$\Phi = \frac{1}{r} Y_l^m(\theta, \phi)\Psi(t, r^*), \tag{4}$$

where r^* denotes the tortoise coordinate

$$r^* \equiv r + 2M\ln(r - 2M). \tag{5}$$

Substitution of Eq. (4) into Eq. (3), with $a = 0$, yields the one-dimensional wave equation

$$[-\partial_{tt} + \partial_{r^*r^*} - V(r)]\Psi(t, r^*) = 0, \tag{6}$$

with the potential $V(r)$ defined by

$$V(r) = \left(1 - \frac{2M}{r}\right)\left[\frac{l(l+1)}{r^2} + \frac{2M}{r^3}\right]. \tag{7}$$

It has been shown, in both numerical and analytic studies [1,3,5], that at a fixed radius the solution of Eq. (6) will fall off as $t^{-(2l+3)}$ for large t and nonstatic initial data.

For $a \neq 0$, it is no longer possible to separate variables and arrive at an equation similar to Eq. (6). While the azimuthal dependence of Φ can still be described by $e^{im\phi}$, a full separation of variables exists only in the frequency domain, as first demonstrated by Brill *et al.* [11]. In this case, both the Teukolsky equation and Eq. (3) admit separable solutions of the form

$$\Phi = e^{-i\omega t} e^{-im\phi}\, {}_sS_l^m(\theta; a\omega) R_{lm}(r; \omega), \tag{8}$$

where ${}_sS_l^m$ are the spin-weight-s spheroidal wave functions. However, since the objective of the present study is the late-time dynamics, a decomposition based on ω modes is not suitable, and one is forced, in principle, to solve a two-dimensional evolution equation for Φ. Nonetheless, the case of slowly rotating black holes circumvents the problem of solving a two-dimensional wave equation.

The use of an azimuthal coordinate defined by asymptotic observers, as is the case with the Boyer-Lindquist ϕ coordinate, introduces unphysical pathologies near the horizon even in the case $a \ll M$. A discussion of those pathologies and their precise manifestation in the slow rotation limit is given in the Appendix. Those coordinate-induced problems are readily dealt with by adopting the Kerr azimuthal coordinate $\tilde{\phi}$ given by

$$d\tilde{\phi} = d\phi + \frac{a}{\Delta} dr. \tag{9}$$

Using the ansatz

$$\Phi \equiv \Psi(t, r^*, \theta) e^{im\tilde{\phi}}, \tag{10}$$

the wave equation (3) yields

$$-\partial_{tt}\Psi - \frac{(r^2+a^2)^2}{\sigma}\partial_{r^*r^*}\Psi + \frac{4\,imarM}{\sigma}\partial_t\Psi - \frac{2[r\Delta + iam(r^2+a^2)]}{\sigma}\partial_{r^*}\Psi - \frac{\Delta}{\sigma}\left[\partial_{\theta\theta}\Psi - \cot\theta\partial_\theta\Psi + \frac{m^2}{\sin^2\theta}\Psi\right] = 0, \tag{11}$$

with

$$\sigma \equiv -(a^2+r^2)^2 + a^2\Delta \sin^2\theta, \tag{12}$$

and the Kerr tortoise coordinate r^* defined by

$$\frac{dr^*}{dr} \equiv \frac{r^2+a^2}{\Delta}. \tag{13}$$

For arbitrary angular momentum per unit mass, $0 \leqslant a \leqslant M$, the angular dependence of Ψ cannot be expressed by $Y_l^m(\theta,\tilde{\phi})$, because, in general, modes belonging to different values of l are coupled. This follows directly from the angular dependence of σ. Only if the initial data are prepared in the form of Eq. (8), is the θ dependence given by ${}_sS_l^m(\theta; a\omega)$ at all times.

To first order in a, however, the angular momentum operator in Eq. (11) is the same as in the Schwarzschild case and the coefficients of the temporal and radial derivatives are independent of θ. Hence, the modes belonging to different l decouple, and, under the assumption $a \ll M$, one can seek a solution of Eq. (3) that possesses an angular dependence given by $Y_l^m(\theta,\tilde{\phi})$ following a procedure similar to that used in deriving Eq. (4). That is, one views the function $\Psi(t,r^*)$ as containing a piece $\Psi_0(t,r^*)$, representing the scalar field in the Schwarzschild background, and a second field $\Psi_1(t,r^*)$ that takes into account the correction due to the rotation of the black hole to first order in a. Thus, the ansatz for the solution of Eq. (3) has the form

$$\Phi = \frac{1}{r} Y_l^m(\theta,\tilde{\phi})[\Psi_0(t,r^*) + a\Psi_1(t,r^*)]. \tag{14}$$

In $(t,r^*,\theta,\tilde{\phi})$ coordinates, substitution of Eq. (14) into the wave equation $\nabla_\mu \nabla^\mu \Phi = 0$ and collecting powers of a yields, after separation of variables, the equation

$$\Box_0 \Psi_0 + a(\Box_0 \Psi_1 - \rho_0) + O(a^2) = 0, \tag{15}$$

where

$$\Box_0 \equiv -\partial_{tt} + \partial_{r^*r^*} - V(r) \tag{16a}$$

and

$$\rho_0 \equiv -\frac{2\,im}{r^4}[-2Mr\partial_t \Psi_0 + r^2 \partial_{r^*}\Psi_0 - (r-2M)\Psi_0]. \tag{16b}$$

The system of equations for Ψ_0 and Ψ_1 is obtained by requiring that the zero and first order terms of this expansion vanish independently: namely,

$$[-\partial_{tt} + \partial_{r^*r^*} - V(r)]\Psi_0 = 0, \tag{17a}$$

$$[-\partial_{tt} + \partial_{r^*r^*} + V(r)]\Psi_1 = \frac{2\,im}{r^4}[-2Mr\partial_t\Psi_0 + r^2\partial_{r^*}\Psi_0 - (r-2M)\Psi_0], \tag{17b}$$

with $V(r)$ given by Eq. (7). As expected, the equation for Ψ_0 does not contain terms depending on Ψ_1, and the source term ρ_0 in the equation for Ψ_1 only depends on the solution Ψ_0 of the zero order equation. The problem has then been reduced to solving the homogeneous equation (17a) for Ψ_0 and using this solution as a source in the inhomogeneous equation (17b).

Owing to the one-way membrane character of the horizon, the use of ingoing wave boundary conditions at the horizon fits most naturally the solution of Eq. (17a). The asymptotic form of Ψ_0 for $r^* \to -\infty$ is then a wave with constant amplitude propagating to the horizon.

As $r^* \to -\infty$, the source term behaves like $\rho_0 \to -\partial_t \Psi_0 + \partial_{r^*}\Psi_0$. Thus, $\rho_0 \to 0$ if $\Psi_0 \to \Psi_0(t+r^*)$. On the other hand, at $r^* \to \infty$, $\rho_0 \to 0$ due to the assumption that Ψ_0 has compact initial data.

III. POWER-LAW TAILS

The numerical results presented here were computed with a second order staggered in time evolution scheme. For consistency, a characteristic numerical integration was also used, and the results were in complete agreement.

In general, both Ψ_0 and Ψ_1 are complex quantities. Owing to the purely imaginary coefficients of $\partial_t\Psi_0$, $\partial_{r^*}\Psi_0$, and Ψ_0 in the source term in Eq. (17b), $\mathrm{Im}\Psi_0$ is coupled to $\mathrm{Re}\Psi_1$, and $\mathrm{Re}\Psi_0$ to $\mathrm{Im}\Psi_1$. Hence, without loss of generality, one may assume $\mathrm{Re}\Psi_0 \equiv \mathrm{Im}\Psi_1 \equiv 0$. Since the separation variable m plays the role of a scaling factor for the source term in Eq. (17b), in the numerical calculations $m = M = 1$ is used.

The initial data for Ψ_0 consist of a bell-shaped pulse propagating outwards given by

$$\Psi_0^{\mathrm{ini}} = c_1\{[c_2(r^*-t) - r^*_{\mathrm{in}}][c_2(r^*-t) - r^*_{\mathrm{out}}]\}^8 \tag{18}$$

for $r^*_{\mathrm{in}} \leqslant r^* \leqslant r^*_{\mathrm{out}}$ and vanishing otherwise. The parameters have been chosen to yield a pulse centered at $r^* = 100$; that is, $c_1 = 100, c_2 = 0.02$, and $r^*_{\mathrm{in,out}} = 1,3$. On the other hand, the initial conditions for Ψ_1 are $\Psi_1 = \partial_t \Psi_1 = 0$. Numerical experiments have shown that the tail behavior is not affected by the choice of initial conditions for Ψ_1.

As previously discussed, the behavior of both the potential and the source term in Eq. (17b) makes it possible, in principle, to impose ingoing boundary conditions at the horizon and outgoing conditions at infinity, i.e. $\lim_{r^* \to \mp\infty} \Psi_{0,1} = \Psi_{0,1}(t \pm r^*)$. However, in a Cauchy evolution, such as the one under consideration, boundary conditions are imposed at a finite distance [13]. Typically, the computational domains used covered $-50 \leqslant r^* \leqslant 2000$ with $\Delta r^* = 0.1$. Since $r^* = -50$ yields $r - 2M \sim 10^{-12}$, imposing the left (ingoing into the black hole) boundary condition at a finite radius r^* turns out to be a suitable approximation; both the potential $V(r)$ and the source ρ_0 are negligible at $r^* = -50$. A different situation is encountered at the right boundary. Even though the potential $V(r)$ and the source ρ_0 vanish as $r^* \to \infty$, at the right boundary ($r^* = 2000$) of the computational domain, and especially for late times, the outgoing boundary condition is not a good approximation. However, this boundary is at a sufficiently large radial distance, so it allows enough dynamical evolution range to obtain the tail behavior before numerical boundary effects contaminate the solution.

Figure 1 shows several snapshots of the evolution for $l = 1$, $0 \leqslant t \leqslant 200$. During the evolution, the initially outgoing

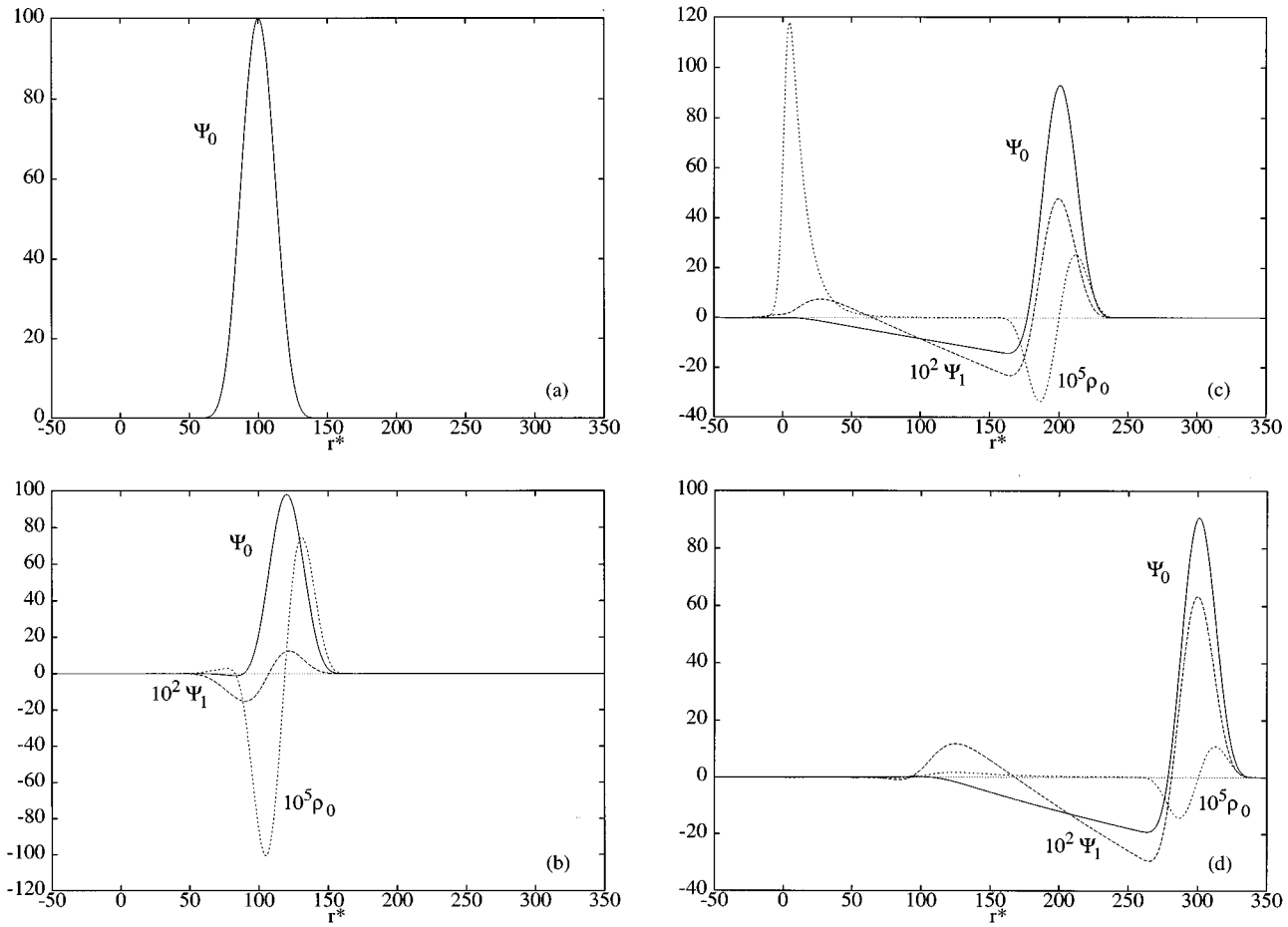

FIG. 1. Evolution of Ψ_0, ρ_0, and Ψ_1 for $l=1$, $0\leqslant t\leqslant 200$. (a) At $t=0$, $\Psi_1=\rho_0=0$. (b) At $t=20$, the source ρ_0 is dominated by the initial shape of Ψ_0. (c) At $t=100$, a peak in ρ_0 has developed due to the part of the initial pulse that was backscattered off the potential and is propagating inwards. (d) At $t=200$, as a consequence of the peak of ρ_0 in (c), a hump appears in the trailing part of Ψ_1.

zero order function Ψ_0 is followed by a pulse in Ψ_1 driven by the source ρ_0. In Fig. 1(a), the initial bell-shaped pulse for Ψ_0 centered at $r^*=100$ is shown ($\Psi_1=\rho_0=0$). At $t=20$, Fig. 1(b) depicts the radial dependence of the source ρ_0 dominated by the initial shape of Ψ_0. As displayed in Fig. 1(c), after an evolution time of $t=100$, a pronounced peak of ρ_0 has developed due to the part of the initial pulse that was backscattered off the potential and is propagating inwards. In Fig. 1(d), at $t=200$, as a consequence of the peak of ρ_0, a hump appears in the trailing part of Ψ_1.

Before presenting the numerical results, a heuristic analytical argument is given, estimating the expected late-time behavior. The argument is based on the result that the late-time decay of waves propagating on curved spacetimes is dictated by the spatial asymptotics of the potential [4]. The argument does not include the contribution from the centrifugal barrier ($l=0$). Starting with the original wave equation (1) one obtains, to first order in a,

$$[-\partial_{tt}+\partial_{r*r*}-V(r)]\Psi+\frac{2\,imaM}{r^3}$$

$$\times\left[-2\,\partial_t+r\,\partial_{r*}+\left(1-\frac{2M}{r}\right)\right]\Psi=0, \tag{19}$$

where

$$\Phi=\Psi(t,r^*)Y_l^m(\theta,\tilde{\phi}).$$

Equation (19) contains two operators: the operator for scalar fields on Schwarzschild background (first term in squared brackets) and a second operator (first order in a) containing first order spatial and temporal derivatives.

If one views the late-time tail behavior at a radial position r, as the result of the scattering by a potential at $\hat{r}\gg r$ of a wave originated at $r_o\sim r$, the arrival time of the scattered wave is approximately given by $t\approx(\hat{r}-r_o)+(\hat{r}-r)\approx 2\hat{r}$ [3]. At late times, the scalar field $\Psi\propto V_T(\hat{r})\approx V_T(t)$, where $V_T(r,t)=V(r)+V_a(r,t)$ represents the ''total'' potential; that is, the Schwarzschild potential (7) with $l=0$ plus a correction V_a due to the rotation of the black hole. This correction arises from the second term in squared brackets in Eq. (19). Under the late-time and large scattering radius approximation, $\partial_t\Psi\sim\Psi/t$ and $\partial_{r*}\Psi\sim\Psi/r$. Thus, $V_a(\hat{r},t)\sim\hat{r}^{-3}+\hat{r}^{-3}t^{-1}+\hat{r}^{-4}\sim t^{-3}$. Therefore, $\Psi\propto V+V_a\sim t^{-3}$ since $V\sim t^{-3}$. This shows that both the Schwarzschild potential and the perturbative potential contribute with the same power-law behavior. The centrifugal barrier adds a t^{-2l} factor to the tails [4].

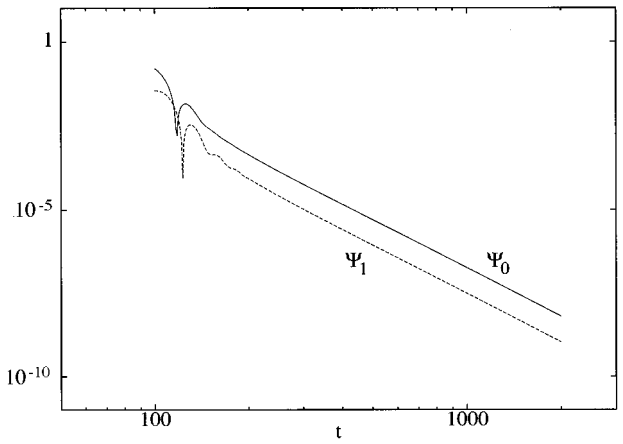

FIG. 2. Log-log plots of Ψ_0 and Ψ_1 for $l=1$ at $r^*=10$. The power-law exponents are -4.93 for Ψ_0 and -4.92 for Ψ_1. The wiggles that can be seen for $t<200$ are remainders of the quasinormal ringing of the black hole.

The numerical investigation of the late-time behavior was performed at different distances from the black hole. Power-law behavior, with an exponent independent of the location of observation, was detected for both Ψ_0 and Ψ_1 for different multipole indices l. As shown in Figs. 2 and 3, the numerically determined power-law exponents for the zero and first order solutions are in good agreement: For $l=1$, the power-law exponents are -4.93 for Ψ_0 and -4.92 for Ψ_1; the theoretically predicted value is 5 for this case. For $l=2$, the exponents are -7.02 and -7.07, respectively, and the corresponding theoretical value is 7. These results lead to a power-law exponent for $\Phi=(1/r)\,Y_l^m[\Psi_0+a\Psi_1]$ that is unchanged with respect to the behavior on a Schwarzschild background.

IV. RAPIDLY ROTATING BLACK HOLES

The next step is to consider the case of rotating black holes with arbitrary angular momentum per unit mass, i.e., $0\leqslant a\leqslant M$. The objective here is to investigate whether the Schwarzschild tail behavior is modified for rapidly rotating black holes. The starting point is the wave equation (3) written in coordinates $(t,r^*,\theta,\tilde{\phi})$. The equation reduces to the flat wave equation $[-\partial_{tt}+\partial_{r^*r^*}]\Psi=0$ for $r^*\to\pm\infty$, thus a simple formulation of radial outgoing boundary conditions is possible.

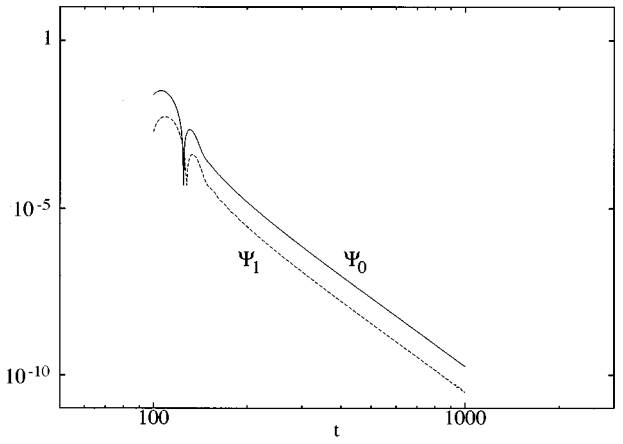

FIG. 3. Log-log plots of Ψ_0 and Ψ_1 for $l=2$ at $r^*=10$. The power-law exponents are given by -7.02 and -7.07, respectively.

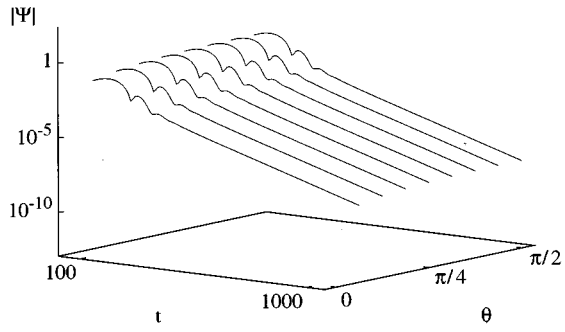

FIG. 4. Log-log plots of $|\Psi|$ for $m=1$, $a=0.99$ at $r^*=10$ for different equidistant angular directions from $\theta=\pi/16$ to $\theta=\pi/2$. The initial angular dependence was given by $\mathrm{Im}\Psi\sim P_1^1\sim\sin\theta$. For large times the time dependence is given by $|\Psi|\sim t^{-\mu}$, where $\mu=4.87\pm0.005$ for all observed angles. The theoretical power-law tail exponent in the Schwarzschild case is given by $\mu=5$.

Equation (11) was evolved on a rectangular spatial grid in $r_{\min}\leqslant r\leqslant r_{\max}$, $0\leqslant\theta\leqslant\pi/2$. The numerical code was tested for convergence and stability. As in the one-dimensional case, the mass of the black hole was set to $M=1$. The inner radial boundary $r_{\min}$ was chosen so that the limit of the flat wave equation was reasonably approximated (cf. Sec. III). The data at $\theta=0,\pi/2$ were updated according to the behavior of the particular mode under consideration. The values of the field at the poles and the equatorial plane were determined by the value of m and the symmetry of the mode with respect to the equatorial plane: For $m=0$, $\partial_\theta\Psi(t,r^*,0)=0$ for all t,r^*. For nonaxisymmetric waves, given by $m\neq0$, $\Psi(0)=0$ for all modes. At the equator, the condition for the modes symmetric to the equatorial plane is given by $\partial_\theta\Psi(\pi/2)=0$ and the antisymmetric modes are characterized by $\Psi(\pi/2)=0$.

The initial data were given by $\mathrm{Re}\Psi=\partial_t\mathrm{Re}\Psi=0$ and, using Eq. (18), $\mathrm{Im}\Psi=\Psi_0^{\mathrm{ini}}P_l^m/\sqrt{r^2+a^2}$, where a particular associated Legendre polynomial P_l^m had to be chosen according to the mode of interest. For fixed m, a mixing of modes

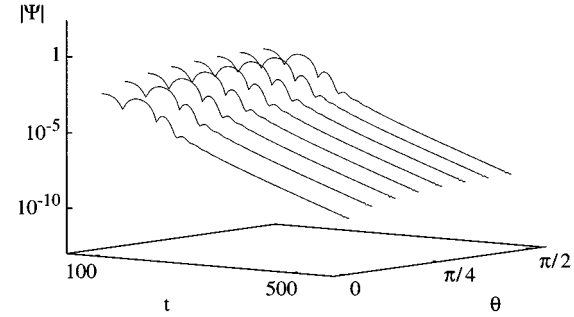

FIG. 5. Same as in Fig. 4, but for $m=2$ and the initial angular dependence given by $\mathrm{Im}\Psi\sim P_2^2\sim\sin^2\theta$. For large times the power-law exponent is $\mu=6.98\pm0.004$ for all observed angles. The theoretical value in the Schwarzschild case is given by $\mu=7$.

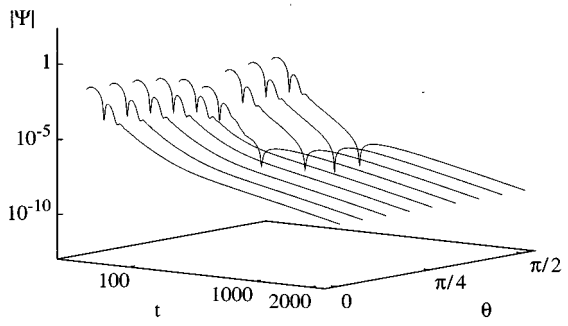

FIG. 6. Log-log plots of $|\Psi|=\mathrm{Im}\Psi$ for $m=0$, $a=0.99$ at $r^*=10$ for different angular directions in equidistant steps from $\theta=0$ to $\theta=\pi/2$. The initial angular dependence was given by $\mathrm{Im}\Psi\sim P_2^0\sim 3\cos^2\theta-1$. Mixing of modes: For large times the time dependence is given by $|\Psi|\sim t^{-\mu}$, where for $\mathrm{Im}\Psi$ the exponent is $2.88\leqslant\mu\leqslant 2.92$ with $\langle\mu\rangle=2.91$ over the observed angles. $\mathrm{Re}\Psi=0$ at all times, because the two equations are decoupled for $m=0$, and $\mathrm{Re}\Psi=(d/dt)\mathrm{Re}\Psi=0$ initially.

belonging to different values of l will occur during the evolution if the initial data do not correspond to the lowest possible mode of l.

In the following figures, the late-time behavior of $|\Psi|$ at $r^*=10$ is displayed for different initial multipoles for an angular momentum parameter of $a=0.99$. Figure 4 shows the late-time behavior for $m=1$. Equidistant angular directions were chosen in the interval from $\theta=\pi/16$ to $\theta=\pi/2$. The initial angular dependence corresponds to $l=m=1$. The late-time behavior can be described by $|\Psi|\sim t^{-\mu}$, where the exponent is given by $\mu=4.87$ for all the displayed angles. In Fig. 5 the analogous situation is shown for $m=2$ and an initial pulse corresponding to $l=m=2$. In this case the power-law exponent for the observed angles is $\mu=6.98$. That is, the power-law exponents governing the late-time behavior for $a=0.99$ do not exhibit a significant change when compared to the Schwarzschild case, in which the theoretical power-law tail exponents are given by $\mu=5$ for $l=m=1$, and $\mu=7$ for $l=m=2$. In both cases the initial pulse used for the two-dimensional evolution is given by the lowest-allowed mode for fixed m.

The situation is different for the case $l=2$, $m=0$, depicted in Fig. 6. Here, the initial pulse is not given by the lowest mode with $m=0$ that is symmetric with respect to the equatorial plane, corresponding to $l=0$. Instead, the initial angular dependence is given by $\mathrm{Im}\Psi\sim P_2^0\sim 3\cos^2\theta-1$. Here, mixing of modes occurs and the late-time evolution is dictated by the lowest mode. The sink on the right-hand side is caused by the transition to the lowest mode. For large times the time dependence is given by $|\Psi|\sim t^{-\mu}$, where $2.88\leqslant\mu\leqslant 2.92$ with $\langle\mu\rangle=2.91$ when averaged over all observed angles. In contrast with this result, the corresponding Schwarzschild case exhibits no mixing of the modes, and the theoretical power-law tail exponent is given by $\mu=7$ for $l=2$, $m=0$.

ACKNOWLEDGMENTS

We thank N. Andersson, R. Gleiser, K. Kokkotas, H.-P. Nollert, J. Pullin, R. Price, and E. Seidel for helpful discussions. This work was supported by the Binary Black Hole Grand Challenge Alliance, NSF PHY/ASC 9318152 (ARPA supplemented) and by NSF Grant Nos. PHY 93-09834 and 93-57219 (NYI) to P.L. W.K. was supported by the Deutscher Akademischer Austauschdienst (DAAD).

APPENDIX

The behavior of the wave equation near the horizon when written in Boyer-Lindquist coordinates is illustrated here, in the context of the slow rotation approximation. The manifestation of this behavior in the solution of the initial value problem is analyzed in the limit $r\to 2M$.

The small a expansion of equation (3) using the ansatz

$$\Phi=\frac{1}{r}Y_l^m(\theta,\phi)[\Psi_0(t,r^*)+a\hat{\Psi}_1(t,r^*)], \tag{A1}$$

yields the system of equations

$$[-\partial_{tt}+\partial_{r^*r^*}-V(r)]\Psi_0=0, \tag{A2a}$$

$$[-\partial_{tt}+\partial_{r^*r^*}-V(r)]\hat{\Psi}_1=i\frac{4mM}{r^3}\partial_t\Psi_0. \tag{A2b}$$

Upon examining equation (A2b) a problematic feature emerges. The source term on the right-hand side does not vanish in the limit $r^*\to-\infty$. More precisely, the asymptotic form of the equation at the horizon is $(-\partial_{tt}+\partial_{r^*r^*})\hat{\Psi}_1=(im/2M^2)\partial_t\Psi_0$. Using null coordinates $v=t+r^*$ and $u=t-r^*$, and assuming a purely ingoing solution $\Psi_0(v)$, one obtains

$$\hat{\Psi}_1(u,v)=b(u)\Psi_0(v)+f_1(v)+f_2(u), \tag{A3}$$

where

$$b(u)=-\frac{im}{8M^2}u, \tag{A4}$$

and f_1, f_2 are solutions of the homogeneous equation.

The presence of this growing mode in the system may at first appear puzzling, since the ansatz (A1) is related to Eq. (14) simply by an angular coordinate redefinition. Yet, the singular nature of the transformation (9) near the horizon is the source of the growing mode. A direct comparison of systems (A2) and (17) reveals that the two sets of equations are equivalent, with $\hat{\Psi}_1$ given by

$$\hat{\Psi}_1(t,r^*)=\Psi_1(t,r^*)+c(r)\Psi_0(t,r^*), \tag{A5}$$

where

$$c(r)=\frac{\pi m}{2M}-\frac{im}{2M}\ln\left(\frac{r}{r-2M}\right). \tag{A6}$$

The solution of Eq. (17b) with the correct source term is denoted by $\Psi_1(t,r^*)$. The coefficient $c(r)$ is singular at the horizon, hence bounded solutions Ψ_0,Ψ_1 give rise to an unbound combination for $\hat{\Psi}_1$. The linear combination (A5) has indeed the horizon blowup demonstrated by Eq. (A3). This follows from the fact that

$$\lim_{r\to 2M} c(r) = \lim_{r\to 2M} b(u) \approx \lim_{r\to 2M} \frac{im}{2M} \ln(r-2M). \tag{A7}$$

An intuitive explanation of this pathology lies in the twisting of azimuthal directions defined at infinity, as seen by an infalling observer near the horizon. The wave evolution is well behaved in a local frame, yet it appears singular in a coordinate system that winds itself infinitely many times around the black hole. The singularity of the evolution in the Boyer-Lindquist coordinates is introduced entirely through this singular (at the horizon) coordinate transformation.

[1] R. H. Price, Phys. Rev. D **5**, 2419 (1972).
[2] C. T. Cunningham, R. H. Price, and V. Moncrief, Astrophys. J. **224**, 643 (1978).
[3] E. S. C. Ching, P. T. Leung, W. M. Suen, and K. Young, Phys. Rev. Lett. **74**, 2414 (1995).
[4] E. S. C. Ching, P. T. Leung, W. M. Suen, and K. Young, Phys. Rev. D **52**, 2118 (1995).
[5] C. Gundlach, R. H. Price, and J. Pullin, Phys. Rev. D **49**, 883 (1994).
[6] R. Gomez and J. Winicour, J. Math. Phys. **33**, 1445 (1992).
[7] C. Gundlach, R. H. Price, and J. Pullin, Phys. Rev. D **49**, 890 (1994).
[8] T. Apostolatos, D. Kennefick, A. Ori, and E. Poisson, Phys. Rev. D **47**, 5376 (1993).
[9] R. H. Price (private communication).
[10] P. Papadopoulos, P. Laguna, and W. Krivan, ''Late-time Behavior of Scalar Fields with Multi-dimensional Potentials'' (in preparation).
[11] D. R. Brill, P. L. Chrzanowski, and C. M. Pereira, Phys. Rev. D **5**, 1913 (1972).
[12] S. A. Teukolsky, Astrophys. J. **185**, 635 (1973).
[13] P. Papadopoulos and P. Laguna, ''Cauchy-Characteristic Evolution of Scalar Waves in a Schwarzschild Space-Time'' (in preparation).